Magnetization and magnetoreflectance in $Zn_{1-x}Mn_xTe$

G. Barilero, C. Rigaux, M. Menant, and Nguyen Hy Hau
Groupe de Physique des Solides de l'Ecole Normale Supérieure, 24 rue Lhomond, 75231 Paris Cédex 05, France

W. Giriat
Centro de Física, Instituto Venezolano de Investigaciones Científicas, Apartado Postal 1827, Caracas 1010A, Venezuela
(Received 13 May 1985)

The exchange splitting of the free-exciton state in $Zn_{1-x}Mn_xTe$ ($x<0.5$) is studied by magnetoreflectance experiments carried out up to 6.5 T, for σ and π light polarization. Magnetization measurements made up to 15 T determine the mean value of the Mn^{2+} spins along the magnetic field. Comparison of magneto-optical with magnetic data, obtained for the same samples, at 1.86 K, in the paramagnetic region ($x\leq 0.17$) shows an excellent agreement with the simple exchange interaction model and yields precise values of exchange integrals of Mn^{2+} ions with conduction and valence electrons (−0.18 and 1.05 eV respectively). Fits of the magnetization data are also described.

I. INTRODUCTION

The ternary random alloys $Zn_{1-x}Mn_xTe$ belong to the family of diluted magnetic semiconductors (DMS). These compounds crystallize in the zinc-blende structure in the composition range $x\leq 0.8$, the Mn^{2+} ions substituting randomly Zn^{2+} at the fcc sublattice sites.[1] This system displays many analogies with $Cd_{1-x}Mn_xTe$ of identical crystal structure. Both systems, however, differ by the values of the lattice parameter (much smaller in $Zn_{1-x}Mn_xTe$ than in $Cd_{1-x}Mn_xTe$ for a given x) and their opposite dependence on composition.[2] While the $Cd_{1-x}Mn_xTe$ system has attracted considerable attention,[3] only few experimental works were recently reported on $Zn_{1-x}Mn_xTe$.[4–8] The magnetic and magneto-optical properties of these compounds are strongly influenced by the localized magnetic moments of $3d^5$ electrons of manganese. Magnetic susceptibility of $Zn_{1-x}Mn_xTe$ was studied over a broad range of temperature (2—250 K) and composition (0.15—0.7).[5] In the paramagnetic region, a Curie-Weiss behavior evidences antiferromagnetic interactions between localized magnetic moments. Above $x\simeq 0.20$, $Zn_{1-x}Mn_xTe$ exhibits a low-temperature spin-glass phase attributed to the frustration of the fcc sublattice.

$Zn_{1-x}Mn_xTe$ are wide-band-gap semiconductors,[6] the energy gap ($E_g=2.38$ eV at 4.2 K for $x=0$) increasing with the Mn composition. Optical absorption studies[7] reveal the existence of several absorption bands below the threshold of the fundamental absorption edge. These absorptions were attributed to intra-ion transitions of Mn^{2+} in the $3d^5$ configuration.

In wide-band-gap zinc-blende DMS, exchange interactions between $3d^5$ electrons of Mn and delocalized electrons induce large spin splittings of Γ_6 and Γ_8 bands in the presence of external magnetic field, resulting in giant splittings of the free-exciton ground state. It was established from magnetic and magneto-optical experiments that the exciton Zeeman splitting is directly proportional to the macroscopic magnetization,[10] in agreement with the mean-field approximation. Previous magnetization and magnetoabsorption studies in $Zn_{1-x}Mn_xTe$ alloys were, however, limited to compounds of low Mn composition.[8]

In this paper we report a systematic study of low-temperature magnetoreflection and magnetization experiments carried out on $Zn_{1-x}Mn_xTe$ compounds in a broad range of composition ($0.03\leq x\leq 0.5$). The exchange splitting of the free-exciton state is studied as a function of magnetic field and composition. Magnetization measurements carried out on the same samples enable the determination of the mean value of the Mn^{2+} spins. Comparison between magneto-optical and magnetization data provides accurate values of exchange integrals for conduction and valence bands.

II. EXPERIMENTS

Single crystals of $Zn_{1-x}Mn_xTe$ were grown by the Bridgman method.[2] With use of high-purity individual elements as starting materials, the binary compounds MnTe and ZnTe were sintered and the proper amount of both compounds were mixed and located in carbonized thick-well quartz tubes. Such tubes, sealed in high vacuum, were placed in a ceramic tube filled with pure argon. Crystallization of $Zn_{1-x}Mn_xTe$ compounds by the Bridgman method was then carried out. This technique provided single crystals of good crystalline quality, but of relatively small dimensions ($10\times 6\times 5$ mm^3). For each investigated sample, the manganese molar fraction was determined by microprobe analysis.

With use of conventional methods, reflectance experiments were carried out in the visible region ($2.38\leq\hbar\omega\leq 2.7$ eV), on samples immersed in superfluid helium, at the temperature $T=1.86$ K. All optical measurements were done on cleaved (110) surfaces. Magnetoreflectivity spectra were obtained in magnetic fields up to 6.5 T, in the Faraday configuration with circular polarization (σ^+,σ^-) and in the Voigt geometry with linearly polarized radiation ($\epsilon||\mathbf{H}$). Ten compounds of Mn composition ranging from 0.03 to 0.5 were studied. Magneti-

TABLE I. Numerical results of magnetization and magnetoreflectance in $Zn_{1-x}Mn_xTe$. x_{opt} is the Mn molar fraction deduced from E_{ex} using the relation (3).

x (%) (microprobe)	x_{opt} (%)	S_0	T_0	x_{eff}/x	$(1-x)^{12}$	$N_0(\beta-\alpha)$ (eV)	$N_0\beta$ (eV)	$N_0\alpha$ (eV)
3.2±0.4	3.2	1.77	1.85±0.15	0.70	0.68	1.19±0.03	1.01	−0.175
3.6±0.4	3.5	1.60	1.85±0.15	0.64	0.65	1.19±0.02	1.02	−0.17
7.4±0.5	7.1	1.18	3.3 ±0.2	0.47	0.42	1.26±0.01	1.07	−0.19
17 ±1	17	0.60	6.5 ±0.5	0.24	0.11	1.26±0.015	1.08	−0.18
25.4±1.5	25.5	0.40	9.8 ±1	0.16	0.03	1.29±0.03	1.10 (±0.02)	−0.19 (±0.008)

zation measurements were carried out by an extraction method on the same samples at the same temperature (1.86 K), in a field up to 15 T, at the Service National des Champs Intenses (Grenoble).

III. MAGNETIZATION

Magnetization measurements were made at $T=1.86$ K in a magnetic field up to 15 T, on $Zn_{1-x}Mn_xTe$ compounds of Mn content $0.03 \leq x \leq 0.25$. Assuming that the magnetization results entirely from Mn^{2+} ions, the mean value of the Mn^{2+} spin component $\langle S_z \rangle$ along the magnetic field is determined from the relation

$$\langle S_z \rangle = M \frac{m(x)}{g\mu_B x N_A} . \quad (1)$$

M is the magnetization per unit mass. $m(x) = (1-x)m_{ZnTe} + x m_{MnTe}$ is the molar mass of the compound $Zn_{1-x}Mn_xTe$, N_A is the Avogadro number. The x values used to determine $\langle S_z \rangle$ are obtained from reflectance data reported in Sec. IV [relation (3)].

Figure 1 shows the magnetic field dependence of $\langle S_z \rangle$ for several Mn compositions. For the lowest content only (3.5%), the magnetization shows a saturation at $H \gtrsim 10$ T. The observed saturation corresponds to the full alignment of the isolated Mn^{2+} spins. By increasing the Mn molar fraction, $\langle S_z \rangle$ decreases due to the formation of antiferromagnetically bound clusters. Experimental magnetization curves are well described by a modified Brillouin function for a spin $S=\frac{5}{2}$, by adjusting the saturation value S_0 and an effective temperature $T_{eff}=T+T_0$, larger than the experimental temperature T:

$$\langle S_z \rangle = -S_0 B_{5/2}(Sg\mu_B H/k_B(T+T_0)) , \quad (2)$$

where $g=2$ and μ_B is the Bohr magneton.

Theoretical fits are reported in Fig. 1, with the parameters $S_0(x)$ and $T_0(x)$ listed in Table I. The saturation value S_0 smaller than $S=\frac{5}{2}$ results from the reduction of the fraction of effective spins contributing to the magnetization at low temperature. The proportion of effective spins x_{eff}/x in each investigated compound estimated from the saturation value $x_{eff}/x = S_0/S$ is very close to the fraction of isolated Mn^{2+} spins $(1-x)^{12}$, given by a random Mn distribution (for $x \leq 7\%$) (Table I).

The relatively isolated spins align in the magnetic field according to the Brillouin function modified by introducing an effective temperature larger than T. The phenomenological parameter T_0 reflects the existence of long-range antiferromagnetic interactions between unfrozen magnetic moments. The values of T_0 obtained from the fits are very close to those obtained for $Cd_{1-x}Mn_xTe$ compounds[10] at $T \sim 1.5$ K, as shown in Fig. 2. The parameter T_0 increases linearly with the composition.

At very high fields $H \geq 13$ T, the magnetization departs

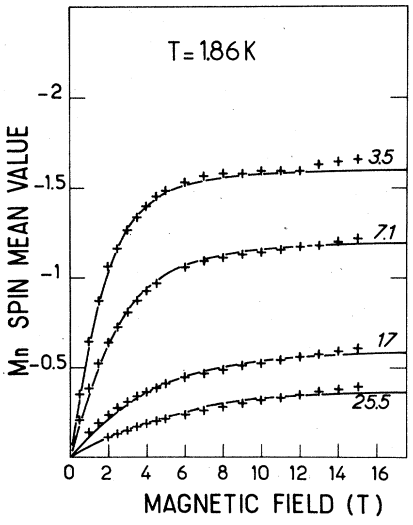

FIG. 1. Mean value of the component of Mn^{2+} spin in $Zn_{1-x}Mn_xTe$ along the magnetic field, obtained from magnetization, at 1.86 K. Compositions are indicated as percents. The continuous lines represent the modified Brillouin function for the parameters S_0 and T_0 listed in Table I.

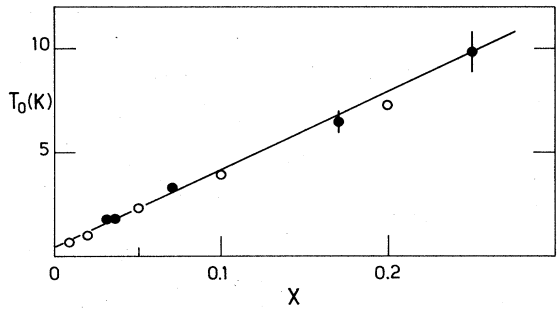

FIG. 2. T_0 vs x for $Zn_{1-x}Mn_xTe$ (solid circles) and $Cd_{1-x}Mn_xTe$ (open circles) [after Gaj *et al.* (Ref. 10)].

from the saturation. This behavior may result from the progressive alignment of Mn^{2+} spins locked in nearest-neighbor antiferromagnetic pairs.

IV. MAGNETOREFLECTANCE

In the absence of magnetic field, a strong reflectivity structure corresponds to the free-exciton ground state associated with valence-to-conduction transitions (Fig. 3). The zero-field exciton energy E_{ex} increases linearly with the Mn content in the composition range $0.03 \leq x \leq 0.5$, as shown in Fig. 4. At $T=1.86$ K, E_{ex} is described by the linear relation deduced from a least-squares fit:

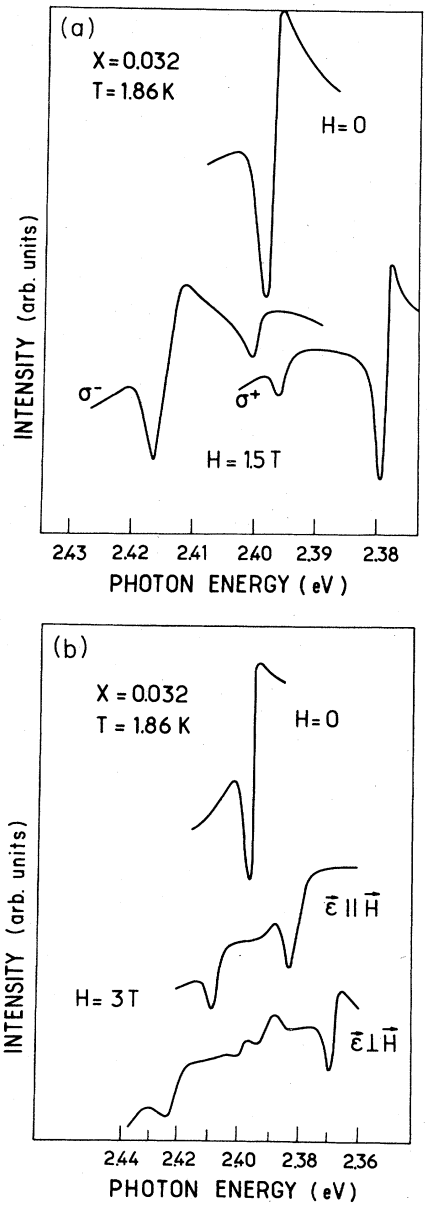

FIG. 3. Magnetoreflectivity spectra of $Zn_{1-x}Mn_xTe$ at 1.86 K. (a) Faraday configuration. Circular polarization. (b) Voigt configuration. Linear polarization.

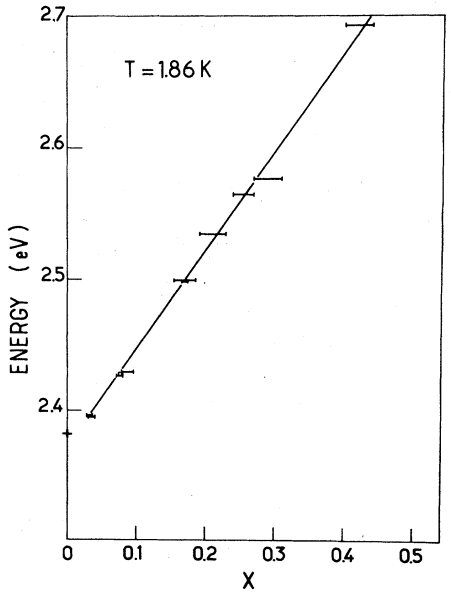

FIG. 4. Energy of the zero-field exciton line versus composition for $Zn_{1-x}Mn_xTe$ compounds. The Mn molar fractions are determined from electron microprobe. The straight line corresponds to the relation (3).

$$E_{ex}=2.372+0.75x \text{ eV} . \quad (3)$$

This relation leads to $E_{ex}=3.12$ eV for cubic MnTe, while the corresponding value obtained from optical measurements in $Cd_{1-x}Mn_xTe$ compounds is 3.18 eV.[10]

In the presence of magnetic field, the exciton ground state exhibits a splitting into six Zeeman-like components, in close analogy with previous experiments on $Cd_{1-x}Mn_xTe$.[11] In the Faraday configuration, a strong and a weak component are observed for each of the circular polarization (σ^+,σ^-). In the Voigt geometry, the spectrum $\epsilon \| \mathbf{H}$ consists of two strong components symmetrically placed with respect to the zero-field structure. Experimental reflectivity data are illustrated in Figs. 3 and 5 for an alloy of low Mn composition ($x=0.032$).

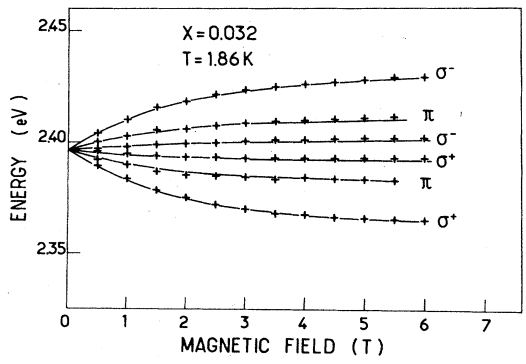

FIG. 5. Energy of the six components of the magnetoreflectance spectrum versus magnetic field for $Zn_{1-x}Mn_xTe$ ($x=0.032$) at $T=1.86$ K. Solid line: calculated energies within the simple model (Ref. 9) for the parameters given in Table I.

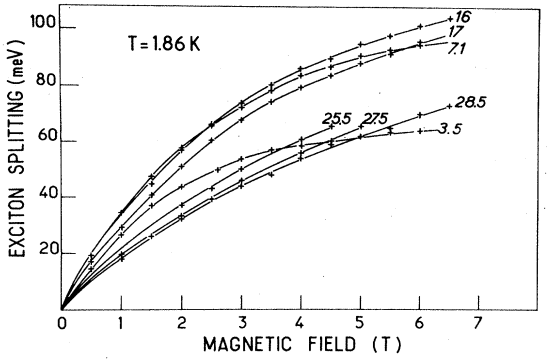

FIG. 6. Splitting of the strong components ΔE_σ^1 versus magnetic field at $T=1.86$ K. Compositions are indicated in percents.

The energy splitting of the strong components (σ polarization) versus magnetic field are reported in Fig. 6, for various compositions.

The observed splitting pattern of the exciton state is well explained within the simplified model developed by Gaj *et al.*[9] for zinc-blende wide-band-gap DMS: in this model, all effects of magnetic field on delocalized electrons are neglected, except the large splittings of the Γ_8 valence ($J=\frac{3}{2}$) and Γ_6 conduction ($J=\frac{1}{2}$) states resulting from the manganese-carrier exchange interactions. The band edges are split by the exchange contributions:

$$E_{\Gamma_6}^{\text{exch}}=xN_0\alpha\langle S_z\rangle m_s \quad (m_s=\pm\tfrac{1}{2}) ,$$

$$E_{\Gamma_8}^{\text{exch}}=\tfrac{1}{3}xN_0\beta\langle S_z\rangle M_J \quad (M_J=\pm\tfrac{3}{2},\pm\tfrac{1}{2}) .$$

α and β are exchange integrals for Γ_6 and Γ_8 bands, respectively. N_0 denotes the number of unit cells per unit volume and x is the Mn molar fraction.

The scheme of magneto-optical transitions is illustrated in Fig. 7. For σ polarization, two strong and two weak transitions are allowed ($M_J-m_s=+1$ for σ^+, $M_J-m_s=-1$ for σ^-); the corresponding energy splittings are

$$\Delta E_\sigma^1=E(\tfrac{3}{2},\tfrac{1}{2})-E(-\tfrac{3}{2},-\tfrac{1}{2})$$
$$=N_0x(\alpha-\beta)\langle S_z\rangle \quad \text{(strong)} , \tag{4}$$

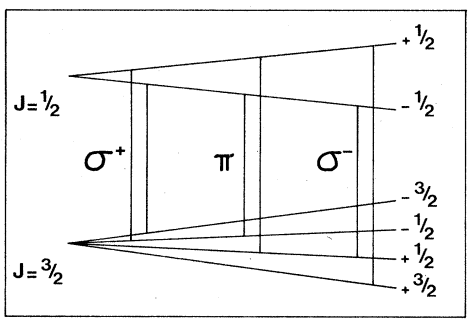

FIG. 7. Scheme of optical transitions between the valence ($J=\frac{3}{2}$) and the conduction ($J=\frac{1}{2}$) electron states.

$$\Delta E_\sigma^2=E(\tfrac{1}{2},-\tfrac{1}{2})-E(-\tfrac{1}{2},\tfrac{1}{2})$$
$$=-N_0x(\alpha+\beta/3)\langle S_z\rangle \quad \text{(weak)} . \tag{5}$$

For π polarization, the energy difference between the allowed transitions ($M_J-m_s=0$) is

$$\Delta E_\pi=E(\tfrac{1}{2},\tfrac{1}{2})-E(-\tfrac{1}{2},-\tfrac{1}{2})=N_0x(\alpha-\beta/3)\langle S_z\rangle . \tag{6}$$

The six components of the reflectance in $Zn_{1-x}Mn_xTe$ are clearly resolved, at 1.86 K, up to $x=0.17$. The ratios of the observed energy splittings $\Delta E_\sigma^2/\Delta E_\sigma^1$ and $\Delta E_\pi/\Delta E_\sigma^1$ are found to be, within experimental accuracy, independent of magnetic field (for $1.5\leq H\leq 6.5$ T), and composition, in agreement with Eqs. (3)—(5). These ratios provide two independent determinations of the ratio of exchange integrals. The most accurate value

$$\alpha/\beta=-0.173\pm0.005 \tag{7}$$

is obtained from the splittings observed for σ polarization. As expected from the model, the exciton Zeeman splittings are directly proportional to the Mn^{2+} spins magnetization. This property was accurately verified for all investigated $Zn_{1-x}Mn_xTe$ compounds by comparing, at various magnetic fields, the splittings of the strong components (Fig. 6) with the $\langle S_z\rangle$ values (Fig. 1). The results are presented in Table I by the values of $N_0(\beta-\alpha)$ obtained from $\Delta E_\sigma^1/x\langle S_z\rangle$ for each Mn composition. Experimental data obtained for all compositions and magnetic fields are reported in Fig. 8.

From (7), the exchange integrals values $N_0\beta$ and $N_0\alpha$ are determined for each Mn content. Values of exchange integrals for various Mn composition are presented in Table I. In the composition range $x\leq 0.25$, the exchange integrals are found within the following limits:

$$N_0\alpha=-0.18\pm0.01 \text{ eV} ,$$

$$N_0\beta=1.05\pm0.06 \text{ eV}$$

for the conduction and valence bands, respectively. These values are in good agreement with the results previously obtained by Twardowski *et al.*[8] in the low composition range.

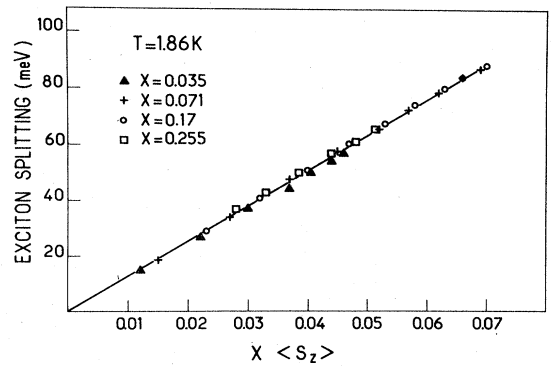

FIG. 8. Splitting of the strong σ components of the exciton line in $Zn_{1-x}Mn_xTe$ plotted versus the mean value per unit cell of the Mn^{2+} spin along the magnetic field.

In conclusion, Mn-carrier exchange interactions described with the simple model[9] fairly well account for the large Zeeman splitting of the exciton state observed by magnetoreflectance for σ and π polarization. The good agreement between calculated and experimental splittings is illustrated in Fig. 5. Precise values of exchange integrals are obtained from simultaneous magnetization and magneto-optical experiments.

ACKNOWLEDGMENTS

We are grateful to Dr. J. C. Picoche and the staff of the Service National des Champs Intenses (Grenoble) for technical assistance in magnetization measurements. We would like to thank Ms. Rommeluere from Centre National de la Recherche Scientifique (Bellevue), who made the electronic microprobe analysis.

[1]A. Pajaczkowska, Prog. Cryst. Growth Charact. **1**, 289 (1978).

[2]W. Giriat and J. K. Furdyna, *Diluted Magnetic Semiconductors,* edited by R. K. Willardson and A. C. Beers (Academic, New York, in press).

[3]J. A. Gaj, J. Phys. Soc. Jpn. Suppl. A **49**, 797 (1980); T. Dietl, *Physics in High Magnetic Fields,* Vol. 24 of *Springer Series in Solid State Sciences,* edited by S. Chikazumi and N. Miura (Spinger, New York, 1981), p. 344; M. Grynberg, Physica **117&118B**, 461 (1983); J. K. Furdyna, J. Appl. Phys. **53**, 7637 (1982); G. Bastard, J. A. Gaj, R. Planel, and C. Rigaux, J. Phys. (Paris) Colloq **41**, C5-247 (1980); J. Mycielski, *Recent Developments in Condensed Matter Physics* (Plenum, New York, 1981), p. 725.

[4]W. Giriat and J. Stankiewicz, Phys. Status Solidi B **124**, K53 (1984).

[5]S. P. Mc Alister, J. K. Furdyna, and W. Giriat, Phys. Rev. B **29**, 1310 (1984).

[6]A. V. Komarov, S. M. Ryabchenko, O. V. Terletskii, I. I. Zheru, and R. D. Ivanchuk, Zh. Exp. Teor. Fiz. **73**, 608 (1977); A. V. Komarov, S. M. Ryabchenko, and N. I. Vitrihovskii, Pisma Zh. Eksp. Teor. Fiz. **27**, 441 (1978).

[7]J. E. Toro, W. M. Becker, B. I. Wang, U. Debska, and J. W. Richardson, Solid State Commun. **52**, 41 (1984).

[8]A. Twardowski, Phys. Lett. **94A**, 103 (1983); A. Twardowski, P. Swiderski, M. Ortenberg, and R. Pauthenet, Solid State Commun. **50**, 509 (1984).

[9]J. A. Gaj, J. Ginter, and R. R. Galazka, Phys. Status Solidi B **89**, 655 (1978).

[10]J. A. Gaj, R. Planel, and G. Fishman, Solid State Commun. **29**, 435 (1978).

[11]J. A. Gaj, P. Byszewski, M. Z. Cieplak, G. Fishman, R. R. Galazka, J. Ginter, M. Nawrocki, Nguyen Th. Khoi, R. Planel, R. Ranvaud, and A. Twardowski, *Proceedings of the 14th International Conference on the Physics of Semiconductors, Edinburgh, 1978,* edited by B. L. H. Wilson (IOP, Bristol, 1978), p.1113.